bioRxiv preprint doi: https://doi.org/10.1101/2023.11.03.565559; this version posted November 3, 2023. The copyright holder for this preprint (which was not certified by peer review) is the author/funder, who has granted bioRxiv a license to display the preprint in perpetuity. It is made available under aCC-BY-NC-ND 4.0 International license.

1 **Nitrate-mediated luminal expansion of *Salmonella* Typhimurium is dependent on the ER**
2 **stress protein CHOP**

3 Short title: CHOP contributes to *Salmonella* growth in the GI tract.

4 Lydia A. Sweet[1], Sharon K. Kuss-Duerkop[1], Mariana X. Byndloss[2], A. Marijke Keestra-
5 Gounder[1]*

6 [1]Department of Immunology and Microbiology, University of Colorado Anschutz Medical Campus,
7 Aurora, CO, USA

8 [2] Howard Hughes Medical Institute, Vanderbilt University Medical Center, Nashville, TN 37232,
9 USA; Department of Pathology, Microbiology, and Immunology, Vanderbilt University Medical
10 Center, Nashville, TN 37232, USA; Vanderbilt Institute of Infection, Immunology, and
11 Inflammation, Vanderbilt University Medical Center, Nashville, TN 37232, USA; Vanderbilt
12 Digestive Disease Center, Vanderbilt University Medical Center, Nashville, TN 37232, USA;
13 Vanderbilt Microbiome Innovation Center, Vanderbilt University, Nashville, TN 37235, USA.

14

15

16 **Keywords**: *Salmonella*, innate immunity, ER stress, CHOP, nitrate

17

18 *Correspondence:

19 Marijke Keestra-Gounder, PhD, Department of Immunology and Microbiology, University of
20 Colorado School of Medicine, Aurora, CO 80045

21 E-mail: Marijke.Keestra-Gounder@cuanschutz.edu

22 Phone: 303-724-8668

bioRxiv preprint doi: https://doi.org/10.1101/2023.11.03.565559; this version posted November 3, 2023. The copyright holder for this preprint (which was not certified by peer review) is the author/funder, who has granted bioRxiv a license to display the preprint in perpetuity. It is made available under aCC-BY-NC-ND 4.0 International license.

23 **Abstract**

24 *Salmonella* Typhimurium is an enteric pathogen that employs a variety of mechanisms to exploit
25 inflammation resulting in expansion in the intestinal tract, but host factors that contribute to or
26 counteract the luminal expansion are not well-defined. Endoplasmic reticulum (ER) stress induces
27 inflammation and plays an important role in the pathogenesis of infectious diseases. However,
28 little is known about the contribution of ER stress-induced inflammation during *Salmonella*
29 pathogenesis. Here, we demonstrate that the ER stress markers *Hspa5* and *Xbp1* are induced in
30 the colon of *S*. Typhimurium infected mice, but the pro-apoptotic transcription factor *Ddit3,* that
31 encodes for the protein CHOP, is significantly downregulated. *S*. Typhimurium-infected mice
32 deficient for CHOP displayed a significant decrease in inflammation, colonization, dissemination,
33 and pathology compared to littermate control mice. Preceding the differences in *S*. Typhimurium
34 colonization, a significant decrease in *Nos2* gene and iNOS protein expression was observed.
35 Deletion of *Chop* decreased the bioavailability of nitrate in the colon leading to reduced fitness
36 advantage of wild type *S*. Typhimurium over a *napA narZ narG* mutant strain (deficient in nitrate
37 respiration). CD11b+ myeloid cells, but not intestinal epithelial cells, produced iNOS resulting in
38 nitrate bioavailability for *S*. Typhimurium to expand in the intestinal tract in a CHOP-dependent
39 manner. Altogether our work demonstrates that the host protein CHOP facilitates iNOS
40 expression in CD11b+ cells thereby contributing to luminal expansion of *S*. Typhimurium via
41 nitrate respiration.

42 **Author Summary**

43 *Salmonella* Typhimurium is a gastroenteric bacterium that replicates to large numbers within the
44 gastrointestinal (GI) tract allowing for efficient host-to-host transmission. One strategy that allows
45 *Salmonella* to expand in the GI tract is via nitrate respiration that is generated during *Salmonella*
46 infections. Our results presented here provide more insight into the role of the host protein CHOP
47 in the production of nitrate and the subsequent growth of *Salmonella* in the GI tract. CHOP

bioRxiv preprint doi: https://doi.org/10.1101/2023.11.03.565559; this version posted November 3, 2023. The copyright holder for this preprint (which was not certified by peer review) is the author/funder, who has granted bioRxiv a license to display the preprint in perpetuity. It is made available under aCC-BY-NC-ND 4.0 International license.

48 expression is regulated within the unfolded protein response (UPR), an adaptive response
49 pathway that is activated when cells are undergoing endoplasmic reticulum (ER) stress. ER stress
50 has been implicated in several infectious and inflammatory diseases; however, little is known
51 about the contribution of ER stress and the UPR during *Salmonella* infections. Here, we
52 demonstrate that *Chop* is downregulated in mice infected with *S*. Typhimurium, and that mice
53 deficient for CHOP have reduced bacterial numbers in the colon, suggesting that downregulation
54 of *Chop* is a host response to resist intestinal colonization by *Salmonella*. Our results further show
55 that CHOP contributes to increased expression of iNOS, responsible for nitrate production,
56 thereby increasing the bioavailability of nitrate that allows for *Salmonella* growth. Altogether, our
57 research provides a better understanding of the contribution of the ER stress protein CHOP in
58 intestinal health and disease.

bioRxiv preprint doi: https://doi.org/10.1101/2023.11.03.565559; this version posted November 3, 2023. The copyright holder for this preprint (which was not certified by peer review) is the author/funder, who has granted bioRxiv a license to display the preprint in perpetuity. It is made available under aCC-BY-NC-ND 4.0 International license.

59 **Introduction**

60 *Salmonella enterica* serovar Typhimurium (*S*. Typhimurium) is a Gram-negative enteric bacterial
61 pathogen that actively induces intestinal inflammation which allows *S*. Typhimurium to
62 outcompete the host microbiota and expand within the gastrointestinal (GI) tract (1, 2). The main
63 virulence factors required for *Salmonella* to induce intestinal inflammation are two type III
64 secretions systems (T3SS) (1-4). The T3SS-1 allows *S*. Typhimurium to invade intestinal
65 epithelial cells (IECs) resulting in the production of cytokines/chemokines, including KC and
66 CCL2, thereby attracting inflammatory phagocytes (macrophages, monocytes, neutrophils and
67 dendritic cells) to the site of infection (3). The T3SS-2 is required for survival and replication within
68 macrophages (5). In addition to the T3SSs, *Salmonella* induces inflammatory responses via
69 Pathogen-Associated Molecular Patterns (PAMPs) that are detected by Pattern Recognition
70 Receptors (PRRs) (6, 7). Early innate immune responses during *S*. Typhimurium infection include
71 the production of an array of chemokines and cytokines such as KC, TNFα, IL-1β and IL-23 (8-
72 10). Intestinal epithelial cells are the predominant producers of neutrophil chemo-attractant KC
73 during *S*. Typhimurium infection (9, 11, 12). TNFα and IL-1β are mainly produced by accumulated
74 inflammatory monocytes and IL-23, produced by dendritic cells, is a crucial cytokine in the
75 development and maintenance of the pro-inflammatory Th17 response (9, 13). In addition to the
76 induction of chemokines and cytokines, *S*. Typhimurium also causes robust expression of *Nos2*.
77 *Nos2* is the gene encoding for inducible nitric oxide (NO) synthase (iNOS) that catalyzes the
78 production of nitric oxide from L-arginine. Nitric oxide radicals react with superoxide radicals which
79 leads to the generation of nitrate (NO_3^-). Nitrate enhances the growth of *S*. Typhimurium via nitrate
80 respiration (14, 15). It was demonstrated that different cells in the intestinal tract produce nitrate,
81 but interestingly, only the nitrate produced by phagocytic infiltrates is utilized by *S*. Typhimurium
82 (16, 17).

bioRxiv preprint doi: https://doi.org/10.1101/2023.11.03.565559; this version posted November 3, 2023. The copyright holder for this preprint (which was not certified by peer review) is the author/funder, who has granted bioRxiv a license to display the preprint in perpetuity. It is made available under aCC-BY-NC-ND 4.0 International license.

83 Upon infection, the intestinal tract must cope with diverse cellular stresses and as a response,
84 cells activate mechanisms to support cellular functions to adapt to changing environmental
85 conditions. Activation of the unfolded protein response (UPR) is one such mechanism that is
86 induced upon endoplasmic reticulum (ER) stress (18). The ER is a highly dynamic organelle that
87 exerts a major role in coordinating signaling pathways to ensure cellular homeostasis. The ER is
88 the site of synthesis and folding of proteins; however, under different stressful pathological and
89 physiological conditions, the ER is unable to maintain homeostasis and activates the UPR (18).
90 Three transmembrane receptors, ATF6, PERK and IRE1α, are activated and regulate biological
91 processes such as inhibition of protein translation, autophagy, and inflammation to restore cellular
92 homeostasis. Under homeostatic conditions, the chaperone BiP, encoded by the *Hspa5* gene, is
93 bound to these receptors, thereby preventing their activation. Perturbation of the ER triggers the
94 release of BiP from ATF6, PERK and IRE1α, resulting in dimerization and phosphorylation of
95 these receptors to an active state (18). ATF6, PERK and IRE1α subsequently activate the
96 transcription factors ATF6f, ATF4 and XBP1, respectively, which then bind to ER stress elements
97 (ERSE) that result in the transcription of genes such as *Hspa5*, *Xbp1*, and *Ddit3* (herein referred
98 to as *Chop*), the gene encoding transcription factor CCAAT/enhancer-binding protein homologous
99 protein (CHOP) (18). CHOP is a downstream apoptosis-promoting target of the PERK-ATF4
100 pathway, resulting in ER stress-induced cell death when the ER stress is severe and/or prolonged
101 (19). Although the role of CHOP has focused mostly on the induction of cell death, more recent
102 studies have reported a role for CHOP in regulating inflammation during infections (20, 21).
103 Infection of myeloid cells with *Chlamydia trachomatis* resulted in increased *Chop* expression and
104 binding of CHOP to the *IL23* promoter (21). Increased expression of *Chop* mRNA and CHOP
105 protein was also detected in trophoblasts infected with *Brucella abortus* (22). Activation of *Chop*
106 during *Listeria monocytogenes* infection was shown to be detrimental to the host leading to
107 increased morbidity and mortality (23). Shiga toxins expressed by enteric pathogens *Shigella*

bioRxiv preprint doi: https://doi.org/10.1101/2023.11.03.565559; this version posted November 3, 2023. The copyright holder for this preprint (which was not certified by peer review) is the author/funder, who has granted bioRxiv a license to display the preprint in perpetuity. It is made available under aCC-BY-NC-ND 4.0 International license.

108 *dysenteriae* 1 and enterohaemorrhagic *Escherichia coli* (EHEC) increased CHOP expression and
109 induced monocytic cell apoptosis (24). Thus, CHOP has a critical, yet not well defined, role during
110 bacterial infections.

111 Although a lot is known about the mechanisms of *Salmonella*-induced intestinal inflammation, not
112 much is known about the contribution of ER stress during *Salmonella* infections. Treatment of
113 *Salmonella*-infected mice with the ER stress inhibitor TUDCA resulted in increased colonization
114 of the small intestine because of decreased lysozyme production mediated by the ER stress-
115 induced secretory autophagy pathway in Paneth cells (25). In HeLa cells, however, it was
116 demonstrated that cells pretreated with the ER stress inducer thapsigargin resulted in increased
117 *Salmonella* replication, suggesting that activation of ER stress provides a favorable environment
118 for *Salmonella* (26). Here, we set out to investigate the involvement of ER stress, and more
119 specifically the function of ER stress-induced CHOP, in the *Salmonella*-induced colitis model as
120 well as the contribution of CHOP to inflammation, colon pathology and luminal expansion of S.
121 Typhimurium.

bioRxiv preprint doi: https://doi.org/10.1101/2023.11.03.565559; this version posted November 3, 2023. The copyright holder for this preprint (which was not certified by peer review) is the author/funder, who has granted bioRxiv a license to display the preprint in perpetuity. It is made available under aCC-BY-NC-ND 4.0 International license.

122 **Results**

123 **Activation of the ER stress response during *S.* Typhimurium infection**

124 To investigate whether the ER stress response is activated in the colon during infection we
125 infected streptomycin pretreated mice with *S*. Typhimurium SL1344 and humanely euthanized the
126 mice at 24, 48 and 72 hr post infection. Expression of the UPR target genes *Xbp1* and *Hspa5* are
127 significantly upregulated in the colon of infected mice at all time points tested, indicating the ER
128 stress response is activated during infection (Figure 1A and B). In contrast, *Chop* is significantly
129 downregulated at day 72h post infection (Figure 1C). These results suggest that ER stress is
130 activated during *Salmonella* infection, but that activation of the three UPR branches may be
131 differentially regulated during intestinal inflammation.

132

133 ***Chop$^{-/-}$* mice have reduced *S.* Typhimurium colonization, dissemination and tissue**
134 **pathology.**

135 The dissociation between UPR activation and reduced *Chop* expression in *Salmonella*-infected
136 colonic tissue was surprising, since it has been demonstrated previously that other bacterial
137 pathogens induce the expression of *Chop* (21-25). To investigate the role of CHOP during
138 *Salmonella* infections, we infected CHOP deficient mice (*Chop$^{-/-}$*)*,* heterozygous (*Chop$^{+/-}$*) and
139 wildtype (*Chop$^{+/+}$*) control mice with *S*. Typhimurium SL1344. Expression of *Xbp1* and *Hspa5* was
140 not significantly different in *Chop$^{-/-}$* mice compared to the control mice, indicating ER stress is
141 induced in CHOP deficient mice (Figure S1A and B). Importantly, no significant differences in
142 colon colonization and dissemination to the liver were observed when comparing heterozygous
143 (*Chop$^{+/-}$*) and wildtype (*Chop$^{+/+}$*) mice (Figure S1C and D). We therefore continued using
144 heterozygous *Chop$^{+/-}$* littermate control mice in comparison with *Chop$^{-/-}$* mice for consecutive
145 experiments. The *Chop$^{-/-}$* mice, on the other hand, had significantly lower bacterial numbers in the
146 colon and liver 72hr post infection (Figure 2A and B). At 72hr post infection the *Chop$^{-/-}$* mice had

bioRxiv preprint doi: https://doi.org/10.1101/2023.11.03.565559; this version posted November 3, 2023. The copyright holder for this preprint (which was not certified by peer review) is the author/funder, who has granted bioRxiv a license to display the preprint in perpetuity. It is made available under aCC-BY-NC-ND 4.0 International license.

147 significantly reduced histopathology scores and neutrophil counts (Figure 2C-E). There were no
148 significant differences in histopathology scores between the *Chop*$^{-/-}$ mice and the littermate control
149 mice at 48hr post infection (Figure S2).

150

151 **CHOP contributes to the expression of pro-inflammatory cytokines during *S.* Typhimurium**
152 **infection.**

153 *S*. Typhimurium utilizes inflammation to drive bacterial expansion, suggesting that the reduced
154 bacterial burdens and histopathology at 72h p.i. may be linked to a decrease in the inflammatory
155 response (2) (Figure 2). At 24 hours post-infection we observed decreased expression of *Nos2*
156 and *Tnfa* in the colon of *Chop*$^{-/-}$ mice suggesting that CHOP has a role in the induction of
157 inflammation (Fig. 3A and B). We did not observe any differences at basal level in mock-infected
158 *Chop*$^{-/-}$ mice and littermate control mice (data not shown). At the later time points, *Nos2* and *Tnfa*
159 expression remained decreased and *Il1b, Kc*, and *Il23* were also reduced (Figure 3). The reduced
160 gene expression at 24 and 48hr post infection was not the result of reduced bacterial numbers in
161 the colon, since the difference in colon colonization was observed only at 72hr post infection
162 (Figure 2A and B).

163

164 ***Chop*$^{-/-}$ mice have reduced iNOS expression leading to decreased colon colonization**

165 *Nos2* encodes the inducible nitric oxide synthase (iNOS), which is present at lower levels in the
166 colon of *Chop*$^{-/-}$ mice 48hr after infection with *S*. Typhimurium (Figure S3A). The reduced
167 expression of *Nos2* mRNA and iNOS protein is of particular interest, because iNOS has been
168 implicated in enhanced nitrate production in the intestinal lumen, thereby contributing to *S*.
169 Typhimurium replication via nitrate respiration (14, 15). To investigate whether deletion of *Chop*
170 would decrease the bioavailability of nitrate in the colon, *Chop*$^{-/-}$ and heterozygous control mice

bioRxiv preprint doi: https://doi.org/10.1101/2023.11.03.565559; this version posted November 3, 2023. The copyright holder for this preprint (which was not certified by peer review) is the author/funder, who has granted bioRxiv a license to display the preprint in perpetuity. It is made available under aCC-BY-NC-ND 4.0 International license.

171 were infected with a 1:1 mixture of wild type SL1344 and a nitrate respiration-deficient strain
172 (*napAnarGnarZ*) (15). At 48hr and 72hr post infection mice were sacrificed and CFUs in the colon
173 contents enumerated. The fitness advantage conferred to the wild type SL1344 by nitrate
174 respiration was significantly diminished in the *Chop*$^{-/-}$ mice at 72hr, but not at 48hr post infection
175 (Figure 4 and Figure S3B). These results suggest a role for CHOP in the production of nitrate
176 resulting in the growth benefit for *S*. Typhimurium via nitrate respiration.
177

178 **CHOP expression in intestinal epithelial cells does not contribute to *S.* Typhimurium**
179 **pathogenesis.**

180 Previous studies with mouse models of T-cell-mediated and bacteria-driven colitis have
181 demonstrated that both CHOP mRNA and protein expression is downregulated in intestinal
182 epithelial cells (27). To investigate whether CHOP expression in IECs results in increased
183 *Salmonella* burden we infected *Chop*$^{\Delta IEC}$ mice and littermate control mice (*Chop*^{flox}) with *S.*
184 Typhimurium. At 48hr and 72hr post infection we did not observe any significant differences in
185 colon colonization or dissemination to the liver (Figure 5A and B, and Figure S4A and B).
186 Moreover, no differences were observed in histopathology scores or neutrophil counts (Figure 5C
187 and D, and Figure S4C and D), suggesting that CHOP expression in IECs does not contribute to
188 *Salmonella* expansion or pathology in the intestinal tract. Additionally, we did not observe
189 significant differences in gene expression of *Kc*, *Il1b*, *Tnfa* and *Il23* (Figure S4 and S5). More
190 importantly, no differences were observed in the expression of *Nos2* (Figure 5E), indicating that
191 CHOP in IECs does not contribute to nitrate production required for *Salmonella* growth in the
192 intestinal lumen.

193

194 **iNOS expression in CD11b+ colonic cells is dependent on CHOP**

bioRxiv preprint doi: https://doi.org/10.1101/2023.11.03.565559; this version posted November 3, 2023. The copyright holder for this preprint (which was not certified by peer review) is the author/funder, who has granted bioRxiv a license to display the preprint in perpetuity. It is made available under aCC-BY-NC-ND 4.0 International license.

195 It was demonstrated that inflammatory phagocytes produce nitrate which is utilized by S.
196 Typhimurium (16, 17). To investigate whether CHOP expression in myeloid cells contributes to
197 the production of nitrate, flow cytometric analysis was performed on live colonic cells for the
198 expression of iNOS (Figure 6A). Isolated live cells were gated for a population that was positive
199 for the leucocyte marker CD45 and positive for CD11b, the marker for inflammatory phagocytes
200 (i.e. monocytes/macrophages, neutrophils). There were no significant differences in the
201 percentage of CD45+/CD11b+/iNOS- cells isolated from *S.* Typhimurium infected *Chop*$^{-/-}$ mice
202 compared to littermate control mice (Figure 6B), suggesting CHOP expression is not required for
203 recruitment of CD11b+ cells. Infected *Chop*$^{-/-}$ mice, however, have a lower percentage of live
204 CD45+/CD11b+ cells that were iNOS+ compared to infected littermate control mice, indicating
205 that CHOP expression in CD11b+ cells contribute to iNOS production (Figure 6C). Consistent
206 with this finding, flow cytometric analysis disclosed that the total number of CD45+/CD11b+/iNOS-
207 cells from the colon of infected *Chop*$^{-/-}$ and littermate control mice was not significantly different,
208 but *Chop*$^{-/-}$ mice have significantly lower numbers of CD45+/CD11b+/iNOS+ cells (Figure 6D and
209 E). Overall, our data demonstrate that CHOP contributes to iNOS expression in CD45+/CD11b+
210 colonic cells, resulting in increased nitrate availability that *S.* Typhimurium utilizes for respiration
211 during infection.

212

213 **Discussion**

214 ER stress and activation of the UPR play major roles in the pathology and resolution of bacterial
215 infections (24, 28-30). Our work expands on the role of ER stress during *S.* Typhimurium infection
216 and indicates that CHOP promotes luminal expansion in the colon via nitrate respiration derived
217 from CD45+CD11b+ cells. Bel *et al* demonstrated that *S.* Typhimurium infection increased CHOP
218 expression in the small intestine, contrary to our finding of *Chop* downregulation in colonic tissues.
219 Activation of ER stress by *S.* Typhimurium in Paneth cells in the mouse small intestine resulted

bioRxiv preprint doi: https://doi.org/10.1101/2023.11.03.565559; this version posted November 3, 2023. The copyright holder for this preprint (which was not certified by peer review) is the author/funder, who has granted bioRxiv a license to display the preprint in perpetuity. It is made available under aCC-BY-NC-ND 4.0 International license.

220 in activation of the secretory autophagy pathway leading to increased lysozyme secretion in the
221 lumen and increased lysozyme mediated killing (25). Treating mice with tauroursodeoxycholic
222 acid (TUDCA), thereby inhibiting the ER stress response, and thus CHOP expression, resulted in
223 increased bacterial numbers in the small intestinal luminal contents and increased dissemination
224 to liver and spleen. TUDCA attenuates ER stress by inhibiting the dissociation of BiP from the
225 receptors and therefore may not only inhibit CHOP expression but also the IRE1α and ATF6
226 pathways, which could contribute to the increased bacterial numbers (31). CHOP protein and
227 *Chop* mRNA is downregulated in colonic tissues derived from mouse models of T-cell-mediated
228 and bacteria-driven colitis (27) and from colonic tissues from ulcerative colitis (UC) patients (32).
229 In DSS- and TNBS-induced colitis, however, CHOP protein and *Chop* mRNA was increased (33).
230 Why CHOP is differentially regulated in a variety of colitis and infection models requires further
231 investigation. Downregulation of CHOP might be a protective mechanism of the host to limit
232 inflammation and/or cell death, whereas upregulation of CHOP may increase inflammation and
233 cell death that could help the host fight off infections. Since *Salmonella* benefits from
234 inflammation, one could argue that the reduced expression of *Chop* in colonic tissue is a protective
235 host response to prevent luminal expansion.

236 Specific deletion of *Chop* from IEC did not contribute to *S.* Typhimurium-induced colitis (Figure
237 5). We observed no differences in pathology, inflammatory responses, or *Salmonella* burdens in
238 colon and liver in *Chop*$^{\Delta IEC}$ mice compared to littermate control mice. In contrast, mice with IEC-
239 specific overexpression of CHOP were more susceptible to DSS-induced colitis, suggesting an
240 important role for CHOP in intestinal epithelial cells during chemically-induced gut inflammation
241 (27). One of the hallmarks of disease in these mice was an increased number of apoptotic IECs
242 compared to wildtype control mice, indicating an important role for CHOP-mediated cell death.
243 Although we did not specifically test for increased IEC apoptosis, *Chop*$^{\Delta IEC}$ mice did not display
244 increased histopathological scores which includes epithelial damage, suggesting that *S.*

bioRxiv preprint doi: https://doi.org/10.1101/2023.11.03.565559; this version posted November 3, 2023. The copyright holder for this preprint (which was not certified by peer review) is the author/funder, who has granted bioRxiv a license to display the preprint in perpetuity. It is made available under aCC-BY-NC-ND 4.0 International license.

245 Typhimurium-induced IEC apoptosis occurs via CHOP-independent mechanisms (34). Our
246 findings, however, do not exclude a role for CHOP in the induction of IEC apoptosis during
247 *Salmonella* infections, as deletion of one cell death pathway may be compensated by other cell
248 death pathways. It has recently been demonstrated that there is an extensive cross-talk between
249 initiators and effectors of distinct cell death pathways, and that loss of a single pathway does not
250 significantly contribute to control of *Salmonella*, but that combined deletion of multiple cell death
251 pathways causes loss of bacterial control in mice (34).

252 Our results revealed that CHOP contributes to the upregulation of several pro-inflammatory
253 mediators, including *Nos2, Kc*, *Il1b*, *Tnfa* and *Il23*. At day 1 and day 2 post infection we observed
254 significantly reduced expression of these cytokines, but no differences in bacterial numbers in
255 colon contents and liver, indicating the reduced gene expression was not a consequence of
256 reduced bacterial numbers. These differences were only observed in infected animals, as there
257 were no significant differences in background expression of these cytokines in uninfected *Chop*$^{-/-}$
258 mice and littermate control mice (data not shown). Since activated macrophages/monocytic
259 infiltrates are capable of secreting KC, IL-1β, TNFα, IL-23 and expressing iNOS, and we excluded
260 a role for IECs, we hypothesized that CHOP plays a role in macrophages by regulating the
261 expression of pro-inflammatory cytokines. Our data demonstrates that CD11b+ cells isolated from
262 colonic tissue of *Chop*$^{-/-}$ infected mice have reduced iNOS expression, suggesting that CD11b+
263 cells, which include macrophages/monocytic infiltrates, contribute to the luminal expansion of *S.*
264 Typhimurium at day 3 post infection. Indeed, the role of monocyte-derived nitrate production in *S.*
265 Typhimurium infection was previously demonstrated. McLaughlin *et al.* showed that mice lacking
266 CCR2, which are unable to recruit monocytes to the intestine, have reduced *Nos2* and iNOS
267 expression and reduced nitrate in the cecal lumen (16). More recently Liou *et al* demonstrated
268 that *S*. Typhimurium does not respire nitrate derived from IEC but rather from inflammatory
269 phagocytes (17). Here, we demonstrate that CHOP contributes to nitrate production and the

bioRxiv preprint doi: https://doi.org/10.1101/2023.11.03.565559; this version posted November 3, 2023. The copyright holder for this preprint (which was not certified by peer review) is the author/funder, who has granted bioRxiv a license to display the preprint in perpetuity. It is made available under aCC-BY-NC-ND 4.0 International license.

270 subsequent replication of *S*. Typhimurium. Furthermore, nitrate bioavailability in the colon of *S*.
271 Typhimurium infected mice is not regulated by CHOP expressed in IEC, suggesting that IEC-
272 derived nitrate does not contribute to nitrate utilization by *S*. Typhimurium which is consistent with
273 the findings from Liou *et al*. Interestingly, intestinal inflammation alters the colonic microbiota,
274 supporting the growth of the Enterobacteriaceae family, which includes *Escherichia coli* (35).
275 Winter *et al.* have demonstrated that one of the underlying mechanisms of growth of *E. coli* in the
276 inflamed GI tract is via nitrate respiration (36), which was later confirmed to be derived from IECs
277 and regulated by Peroxisome proliferator-activated receptor gamma (PPAR-γ) (17, 37). Although
278 we demonstrate that CHOP expression in IECs does not contribute to nitrate respiration by *S*.
279 Typhimurium, this does not exclude the possibility that CHOP does regulate iNOS expression in
280 IECs and that CHOP-mediated epithelial-derived nitrate is utilized by *E. coli*. This could explain a
281 possible mechanism of how CHOP expression in IEC contributes to disease severity in IBD
282 patients as well as in DSS- and TNBS-induced colitis models, and why a bloom of *E. coli*, and not
283 *S*. Typhimurium, is associated with IBD (27, 35, 36, 38).

284 How CHOP controls the expression of iNOS and a variety of cytokines remains to be elucidated.
285 CHOP is a transcription factor and thus might be able to directly influence the transcription of
286 cytokines (21). Alternatively, CHOP may control the expression of pro-inflammatory mediators
287 indirectly by altering the polarity of macrophages (39). Classically activated macrophages (CAM
288 or M1 macrophages) produce excessive quantities of the pro-inflammatory cytokines IL-1, TNFα,
289 and IL-23 as well as increased iNOS expression, whereas alternatively activated macrophages
290 (AAM or M2 macrophages) have characteristics of attenuating inflammation (40). It was
291 demonstrated that CHOP plays a role in polarization of adipose tissue macrophages. High fat diet
292 (HFD) feeding of *Chop*$^{-/-}$ mice skewed the recruitment of infiltrating macrophages more towards
293 a M2 phenotype compared to wild type control mice on a HFD (39). This raises the intriguing
294 thought that downregulation of CHOP might not be a protective host response but might be

bioRxiv preprint doi: https://doi.org/10.1101/2023.11.03.565559; this version posted November 3, 2023. The copyright holder for this preprint (which was not certified by peer review) is the author/funder, who has granted bioRxiv a license to display the preprint in perpetuity. It is made available under aCC-BY-NC-ND 4.0 International license.

295 actively controlled by *Salmonella* to increase M2 macrophages which are metabolically different
296 than M1 macrophages and more favorable for *Salmonella* for long-term persistence (41, 42).

297 The polarization of macrophages might be mediated via CHOP repression of PPAR-γ activation.
298 In IECs it has been demonstrated that ER stress-induced CHOP can act as a repressor of PPAR-
299 γ by sequestering the transcription factor C/EBPβ to prevent it from binding to the promoter region
300 of PPAR-γ, resulting in an increased inflammatory response (43). PPAR-γ activation suppresses
301 the immune state of macrophages by repressing transcription of inflammatory mediators including
302 *Nos2*, *Tnfa*, and *IL1b*. Therefore, in the absence of CHOP, increased PPAR-γ signaling allows for
303 reduced cytokine and *Nos2* expression and subsequently reduced levels of nitrate that can be
304 utilized by Enterobacteriaceae for anaerobic respiration (37).

305 In summary, our results expand on the role of CHOP in the induction of intestinal inflammation
306 during *S*. Typhimurium infection which increases bacterial expansion through increased nitrate
307 bioavailability. Although expression of the ER target genes *Hspa5* and *Xbp1* are increased, *Chop*
308 mRNA expression is reduced in colonic tissues during *S.* Typhimurium infection, suggesting that
309 downregulation of *Chop* might be regarded as a protective host response mechanism, since
310 *Chop*$^{-/-}$ mice have reduced histopathology and *S*. Typhimurium growth. Overall, we demonstrate
311 that the host factor CHOP drives the production of nitrate from CD11b+ cells, which is utilized by
312 *Salmonella* to expand in the intestinal tract.

bioRxiv preprint doi: https://doi.org/10.1101/2023.11.03.565559; this version posted November 3, 2023. The copyright holder for this preprint (which was not certified by peer review) is the author/funder, who has granted bioRxiv a license to display the preprint in perpetuity. It is made available under aCC-BY-NC-ND 4.0 International license.

313 **Materials and Methods**

314 **Mice**

315 *Chop*$^{-/-}$ (B6.129S(Cg)-Ddit3$^{tm2.1Dron}$/J, strain 005530) mice and wild-type C57BL/6 mice were
316 purchased from Jackson laboratory. *Chop*$^{-/-}$ mice were bred with wildtype mice to generate *Chop*$^{+/-}$
317 mice and then *Chop*$^{+/-}$ mice were bred with *Chop*$^{-/-}$ mice to get *Chop*$^{+/-}$ and *Chop*$^{-/-}$ littermates for
318 experiments. *Chop*$^{fl/fl}$ (B6.Cg-Ddit3$^{tm1.1Irt}$/J, strain 030816) and Villin-Cre (B6.Cg-Tg(Vil1-
319 cre)997Gum/J, strain 004586) mice were purchased from Jackson laboratory. *Chop*$^{fl/fl}$ and Villin-
320 Cre mice were bred together to generate *Chop*$^{fl/fl}$ Cre- and *Chop*$^{fl/fl}$ Cre+ littermate mice. All mice
321 were genotyped using protocols and primers from The Jackson Laboratory.

322 ***Salmonella* Typhimurium Infection**

323 Male and female mice (6-10 weeks of age) were pre-treated with 20 mg of streptomycin in 100
324 μL of water by oral gavage 24 hours before infection. Mice were infected with 10^8 CFU SL1344 in
325 100 μL LB broth or mock infected with 100 μL LB broth via oral gavage. Mice were weighed daily
326 and sacrificed at 24-, 48-, or 72-hours post-infection. At the time of sacrifice liver and colon
327 contents were collected for bacterial enumeration. Samples for enumeration were homogenized,
328 serially diluted, and plated on plates containing the appropriate antibiotics. Portions of the colon
329 tissue were snap frozen in liquid nitrogen for RNA and protein extraction. Sections of colon tissue
330 were also collected for histology. For competitive index experiments, mice were infected with
331 $5x10^7$ of *S*. Typhimurium SL1344 Kan^r and $5x10^7$ of *S*. Typhimurium *narG narZ napA* Kan^r Carb^r
332 in 100 μL LB broth. Colon contents were collected for plating and antibiotic selection was used to
333 determine the colonization level for each strain. All mouse experiments were approved by the
334 Institutional Animal Care and Use Committees at the University of Colorado Anschutz Medical
335 Campus.

336 **Quantitative Reverse Transcription-PCR**

bioRxiv preprint doi: https://doi.org/10.1101/2023.11.03.565559; this version posted November 3, 2023. The copyright holder for this preprint (which was not certified by peer review) is the author/funder, who has granted bioRxiv a license to display the preprint in perpetuity. It is made available under aCC-BY-NC-ND 4.0 International license.

337 RNA was isolated from colon tissue using TRI Reagent (Molecular Research Center) according
338 to the manufacturer's instructions. Reverse transcription was performed using 1 μg of DNase-
339 treated RNA (TURBO DNA-free Kit) with TaqMan Reverse Transcription Reagents (Applied
340 Biosystems). Real-time PCR was performed using SYBR Green PCR Master Mix (Applied
341 Biosystems) and the Quantstudio 7 Flex real-time PCR system (Applied Biosystems). Fold
342 change in mRNA levels was calculated using the delta-delta comparative threshold cycle (Ct)
343 method. All targets were normalized to expression levels of *Gapdh* (Table 2. Primer sequences
344 used for qRT-PCR).

345 **Western Blot Analysis**

346 For protein extraction from tissue samples, tissue pieces were snap frozen in liquid nitrogen at
347 the time of harvest. RIPA buffer (10 mM Tris HCl, 1 mM EDTA, 1% Triton X-100, 0.1% Sodium
348 deoxycholate, 0.1% SDS, 140 mM Sodium chloride, 1mM Phenylmethylsulfonyl fluoride, protease
349 inhibitor cocktail (Roche)) was added to tissue samples and samples were homogenized using a
350 bead beater and put on ice to lyse for 1 hour. The tissue lysate was centrifuged at 13000 rpm for
351 15 minutes at 4°C and supernatants containing the proteins were transferred to fresh tubes.
352 Protein concentration was measured using the Pierce BCA protein assay kit according to the
353 manufacturer's instructions. 30 μg of each sample was run on a 10% SDS-PAGE gel for 1 hour
354 at 150 volts. Proteins were transferred to PVDF membrane for 90 minutes at 90 volts. Membranes
355 were then blocked for 1 hour with 5% milk in TBST at RT. Membranes were incubated with anti-
356 iNOS (1:500) and anti-a/b Tubulin (1:5,000) (Cell Signaling Technologies) overnight at 4°C.
357 Secondary anti-rat antibody was used at 1:10,000 for 1 hour at RT. Membranes were developed
358 using ECL Clarity (Bio-Rad) for 4 minutes and then imaged using a G:BOX (Syngene).

359 **Histopathology**

bioRxiv preprint doi: https://doi.org/10.1101/2023.11.03.565559; this version posted November 3, 2023. The copyright holder for this preprint (which was not certified by peer review) is the author/funder, who has granted bioRxiv a license to display the preprint in perpetuity. It is made available under aCC-BY-NC-ND 4.0 International license.

360 Histological samples from mouse experiments were collected in 10% buffered formalin until the
361 time they were embedded, sliced, mounted, and H&E stained by the histology core in Dr. Rubin
362 Tuder's laboratory at the University of Colorado Anschutz Medical Campus. All scoring was done
363 blinded by a veterinary pathologist (Dr. Mariana X. Byndloss at Vanderbilt University). The
364 following pathological changes were scored: (i) neutrophil infiltration, (ii) infiltration by
365 mononuclear cells, (iii) submucosal edema, (iv) epithelial damage, and (v) inflammatory exudate.
366 The pathological changes were scored on a scale from 0 to 4 as follows: 0, no changes; 1,
367 detectable; 2, mild; 3, moderate; 4, severe. Neutrophil counts were determined by high-
368 magnification (x400) microscopy, and numbers were averaged from 10 microscopic fields for each
369 animal.

370 **Single Cell Isolation**

371 After animal sacrifice, the colon was removed and put in ice cold RPMI. Colons were washed with
372 ice cold PBS to remove any contents. The colons were then cut longitudinally and placed in PBS
373 containing 7.5 mM HEPES and 1 mM EDTA (IEL buffer) and shaken at 37°C for 10 minutes.
374 Tissues were then filtered through a 70 μm filter (Fisher Scientific) and put in fresh IEL buffer and
375 shaken for an additional 10 minutes. The samples were filtered again and minced with scissors.
376 Tissues were then digested in RPMI supplemented with 10% FBS, 0.25% β-mercaptoethanol,
377 3.75 mM HEPES, and 0.54 mg/mL type IV collagenase (Worthington) for 30 minutes at 37°C.
378 Digested tissue was then forced through a 70 μm filter and single cells were counted using a C20
379 Automated Cell Counter (Bio-Rad). For staining $3x10^6$ cells were plated in round bottom 96 well
380 plates.

381 **Flow Cytometric Analysis**

382 Single cells suspensions were incubated with anti-CD45 (1:100, Brilliant Violet 785, Biolegend),
383 anti-CD11b (1:50, FITC, Biolegend) and live/dead (1:1000, eFlour 780 Fix Viability, Invitrogen) for

bioRxiv preprint doi: https://doi.org/10.1101/2023.11.03.565559; this version posted November 3, 2023. The copyright holder for this preprint (which was not certified by peer review) is the author/funder, who has granted bioRxiv a license to display the preprint in perpetuity. It is made available under aCC-BY-NC-ND 4.0 International license.

384 30 mins at 4°C. After incubation cold PBS was added to wash cells and samples were spun down
385 at 1500 rpm for 5 minutes. For intracellular staining the Cytofix/Cytoperm kit (BD) was used
386 according to manufacturer's instructions. Briefly, fixation/permeabilization solution was added and
387 cells were then incubated for 20 minutes at 4°C. Cells were then washed using perm/wash buffer
388 to remove fixation solution. Cells were then stained with anti-iNOS (1:100, PE, Invitrogen) for 30
389 minutes at 4°C and then washed using perm/wash buffer. Single stained controls for
390 compensation were done using anti-rat and anti-hamster Igκ/negative control beads (BD). Cell
391 staining was analyzed using LSRFortessa X-20 cell analyzer (BD) at the CU | AMC ImmunoMicro
392 Flow Cytometry Shared Resource. Flow analysis was then performed using FlowJo (BD).

393 **Statistical Analysis**

394 Data analysis was performed with GraphPad PRISM. Data is shown as mean ± standard error of
395 the mean (SEM) or min to max. One-way ANOVAs, Student's t-tests, and Mann-Whitney U tests
396 were performed. More information about statistical analysis can be found in individual figure
397 legends.

398

399 **Acknowledgements**

400 We would like to thank Andreas Baumler (University of California Davis) for providing the *S.*
401 Typhimurium Kan^r and *S.* Typhimurium *narG narZ napA* Kan^r Carb^r strains (15). This work was
402 funded by grants from the NIAID under Award Numbers AI164154 and AI173121, and the
403 University of Colorado start-up funds to A.M.K.G.

404

405 **Author Contributions**

bioRxiv preprint doi: https://doi.org/10.1101/2023.11.03.565559; this version posted November 3, 2023. The copyright holder for this preprint (which was not certified by peer review) is the author/funder, who has granted bioRxiv a license to display the preprint in perpetuity. It is made available under aCC-BY-NC-ND 4.0 International license.

406 L.A.S. and A.M.K.G wrote the manuscript. L.A.S. and A.M.K.G. designed experiments and L.A.S.
407 and S.K.K.D performed the experiments. M.X.B. scored pathological changes. All authors
408 commented on the manuscript.

409

410 **Competing Financial Interest**

411 The authors declare no competing financial interest.

bioRxiv preprint doi: https://doi.org/10.1101/2023.11.03.565559; this version posted November 3, 2023. The copyright holder for this preprint (which was not certified by peer review) is the author/funder, who has granted bioRxiv a license to display the preprint in perpetuity. It is made available under aCC-BY-NC-ND 4.0 International license.

412 **References**
413

414 1. Winter SE, Thiennimitr P, Winter MG, Butler BP, Huseby DL, Crawford RW, et al. Gut inflammation
415 provides a respiratory electron acceptor for Salmonella. Nature. 2010;467(7314):426-9.
416 2. Stecher B, Robbiani R, Walker AW, Westendorf AM, Barthel M, Kremer M, et al. Salmonella
417 enterica serovar typhimurium exploits inflammation to compete with the intestinal microbiota. PLoS Biol.
418 2007;5(10):2177-89.
419 3. Santos RL, Raffatellu M, Bevins CL, Adams LG, Tukel C, Tsolis RM, et al. Life in the inflamed
420 intestine, Salmonella style. Trends Microbiol. 2009;17(11):498-506.
421 4. Tsolis RM, Adams LG, Ficht TA, Baumler AJ. Contribution of Salmonella typhimurium virulence
422 factors to diarrheal disease in calves. Infect Immun. 1999;67(9):4879-85.
423 5. Jennings E, Thurston TLM, Holden DW. Salmonella SPI-2 Type III Secretion System Effectors:
424 Molecular Mechanisms And Physiological Consequences. Cell Host Microbe. 2017;22(2):217-31.
425 6. Mastroeni P, Bryant C. Cytokines in Salmonellosis. EcoSal Plus. 2004;1(1).
426 7. Keestra-Gounder AM, Tsolis RM, Baumler AJ. Now you see me, now you don't: the interaction of
427 Salmonella with innate immune receptors. Nat Rev Microbiol. 2015;13(4):206-16.
428 8. Keestra AM, Godinez I, Xavier MN, Winter MG, Winter SE, Tsolis RM, et al. Early MyD88-
429 Dependent Induction of Interleukin-17A Expression during Salmonella Colitis. Infection and Immunity.
430 2011;79(8):3131-40.
431 9. Godinez I, Keestra AM, Spees A, Baeumler AJ. The IL-23 axis in Salmonella gastroenteritis. Cellular
432 Microbiology. 2011;13(11):1639-47.
433 10. Godinez I, Raffatellu M, Chu H, Paixao TA, Haneda T, Santos RL, et al. Interleukin-23 orchestrates
434 mucosal responses to Salmonella enterica serotype Typhimurium in the intestine. Infect Immun.
435 2009;77(1):387-98.
436 11. Rydstrom A, Wick MJ. Monocyte and neutrophil recruitment during oral Salmonella infection is
437 driven by MyD88-derived chemokines. Eur J Immunol. 2009;39(11):3019-30.
438 12. Zhang S, Kingsley RA, Santos RL, Andrews-Polymenis H, Raffatellu M, Figueiredo J, et al. Molecular
439 pathogenesis of Salmonella enterica serotype typhimurium-induced diarrhea. Infect Immun.
440 2003;71(1):1-12.
441 13. Winter SE, Keestra AM, Tsolis RM, Baumler AJ. The blessings and curses of intestinal inflammation.
442 Cell Host Microbe. 2010;8(1):36-43.
443 14. Fang FC, Vazquez-Torres A. Reactive nitrogen species in host-bacterial interactions. Curr Opin
444 Immunol. 2019;60:96-102.
445 15. Lopez CA, Winter SE, Rivera-Chavez F, Xavier MN, Poon V, Nuccio SP, et al. Phage-mediated
446 acquisition of a type III secreted effector protein boosts growth of salmonella by nitrate respiration. mBio.
447 2012;3(3).
448 16. McLaughlin PA, Bettke JA, Tam JW, Leeds J, Bliska JB, Butler BP, et al. Inflammatory monocytes
449 provide a niche for Salmonella expansion in the lumen of the inflamed intestine. PLoS Pathog.
450 2019;15(7):e1007847.
451 17. Liou MJ, Miller BM, Litvak Y, Nguyen H, Natwick DE, Savage HP, et al. Host cells subdivide nutrient
452 niches into discrete biogeographical microhabitats for gut microbes. Cell Host Microbe. 2022;30(6):836-
453 47 e6.
454 18. Walter P, Ron D. The unfolded protein response: from stress pathway to homeostatic regulation.
455 Science. 2011;334(6059):1081-6.
456 19. Li Y, Guo Y, Tang J, Jiang J, Chen Z. New insights into the roles of CHOP-induced apoptosis in ER
457 stress. Acta Biochim Biophys Sin (Shanghai). 2014;46(8):629-40.

bioRxiv preprint doi: https://doi.org/10.1101/2023.11.03.565559; this version posted November 3, 2023. The copyright holder for this preprint (which was not certified by peer review) is the author/funder, who has granted bioRxiv a license to display the preprint in perpetuity. It is made available under aCC-BY-NC-ND 4.0 International license.

458 20. Datta S, Barrera N, Pavicic PG, Jr., Zhao C, Freeman M, Min B, et al. cEBP Homologous Protein
459 Expression in Macrophages Regulates the Magnitude and Duration of IL-6 Expression and Dextran Sodium
460 Sulfate Colitis. J Interferon Cytokine Res. 2015;35(10):785-94.
461 21. Goodall JC, Wu C, Zhang Y, McNeill L, Ellis L, Saudek V, et al. Endoplasmic reticulum stress-induced
462 transcription factor, CHOP, is crucial for dendritic cell IL-23 expression. Proc Natl Acad Sci U S A.
463 2010;107(41):17698-703.
464 22. Byndloss MX, Tsai AY, Walker GT, Miller CN, Young BM, English BC, et al. Brucella abortus Infection
465 of Placental Trophoblasts Triggers Endoplasmic Reticulum Stress-Mediated Cell Death and Fetal Loss via
466 Type IV Secretion System-Dependent Activation of CHOP. mBio. 2019;10(4).
467 23. Valderrama C, Clark A, Urano F, Unanue ER, Carrero JA. Listeria monocytogenes induces an
468 interferon-enhanced activation of the integrated stress response that is detrimental for resolution of
469 infection in mice. Eur J Immunol. 2017;47(5):830-40.
470 24. Parello CS, Mayer CL, Lee BC, Motomochi A, Kurosawa S, Stearns-Kurosawa DJ. Shiga toxin 2-
471 induced endoplasmic reticulum stress is minimized by activated protein C but does not correlate with
472 lethal kidney injury. Toxins (Basel). 2015;7(1):170-86.
473 25. Bel S, Pendse M, Wang Y, Li Y, Ruhn KA, Hassell B, et al. Paneth cells secrete lysozyme via secretory
474 autophagy during bacterial infection of the intestine. Science. 2017;357(6355):1047-52.
475 26. Antoniou AN, Lenart I, Kriston-Vizi J, Iwawaki T, Turmaine M, McHugh K, et al. Salmonella exploits
476 HLA-B27 and host unfolded protein responses to promote intracellular replication. Ann Rheum Dis.
477 2019;78(1):74-82.
478 27. Waldschmitt N, Berger E, Rath E, Sartor RB, Weigmann B, Heikenwalder M, et al. C/EBP
479 homologous protein inhibits tissue repair in response to gut injury and is inversely regulated with chronic
480 inflammation. Mucosal Immunol. 2014;7(6):1452-66.
481 28. Lee SY, Lee MS, Cherla RP, Tesh VL. Shiga toxin 1 induces apoptosis through the endoplasmic
482 reticulum stress response in human monocytic cells. Cell Microbiol. 2008;10(3):770-80.
483 29. George Z, Omosun Y, Azenabor AA, Partin J, Joseph K, Ellerson D, et al. The Roles of Unfolded
484 Protein Response Pathways in Chlamydia Pathogenesis. J Infect Dis. 2017;215(3):456-65.
485 30. de Jong MF, Starr T, Winter MG, den Hartigh AB, Child R, Knodler LA, et al. Sensing of bacterial
486 type IV secretion via the unfolded protein response. mBio. 2013;4(1):e00418-12.
487 31. Yoon YM, Lee JH, Yun SP, Han YS, Yun CW, Lee HJ, et al. Tauroursodeoxycholic acid reduces ER
488 stress by regulating of Akt-dependent cellular prion protein. Sci Rep. 2016;6:39838.
489 32. Treton X, Pedruzzi E, Cazals-Hatem D, Grodet A, Panis Y, Groyer A, et al. Altered endoplasmic
490 reticulum stress affects translation in inactive colon tissue from patients with ulcerative colitis.
491 Gastroenterology. 2011;141(3):1024-35.
492 33. Namba T, Tanaka K, Ito Y, Ishihara T, Hoshino T, Gotoh T, et al. Positive role of CCAAT/enhancer-
493 binding protein homologous protein, a transcription factor involved in the endoplasmic reticulum stress
494 response in the development of colitis. Am J Pathol. 2009;174(5):1786-98.
495 34. Doerflinger M, Deng Y, Whitney P, Salvamoser R, Engel S, Kueh AJ, et al. Flexible Usage and
496 Interconnectivity of Diverse Cell Death Pathways Protect against Intracellular Infection. Immunity.
497 2020;53(3):533-47 e7.
498 35. Lupp C, Robertson ML, Wickham ME, Sekirov I, Champion OL, Gaynor EC, et al. Host-mediated
499 inflammation disrupts the intestinal microbiota and promotes the overgrowth of Enterobacteriaceae. Cell
500 Host Microbe. 2007;2(2):119-29.
501 36. Winter SE, Winter MG, Xavier MN, Thiennimitr P, Poon V, Keestra AM, et al. Host-Derived Nitrate
502 Boosts Growth of E. coli in the Inflamed Gut. Science. 2013;339(6120):708-11.
503 37. Byndloss MX, Olsan EE, Rivera-Chavez F, Tiffany CR, Cevallos SA, Lokken KL, et al. Microbiota-
504 activated PPAR-gamma signaling inhibits dysbiotic Enterobacteriaceae expansion. Science.
505 2017;357(6351):570-5.

bioRxiv preprint doi: https://doi.org/10.1101/2023.11.03.565559; this version posted November 3, 2023. The copyright holder for this preprint (which was not certified by peer review) is the author/funder, who has granted bioRxiv a license to display the preprint in perpetuity. It is made available under aCC-BY-NC-ND 4.0 International license.

506 38. Giaffer MH, Holdsworth CD, Duerden BI. The assessment of faecal flora in patients with
507 inflammatory bowel disease by a simplified bacteriological technique. J Med Microbiol. 1991;35(4):238-
508 43.
509 39. Suzuki T, Gao J, Ishigaki Y, Kondo K, Sawada S, Izumi T, et al. ER Stress Protein CHOP Mediates
510 Insulin Resistance by Modulating Adipose Tissue Macrophage Polarity. Cell Rep. 2017;18(8):2045-57.
511 40. Murray PJ, Wynn TA. Protective and pathogenic functions of macrophage subsets. Nat Rev
512 Immunol. 2011;11(11):723-37.
513 41. Saliba AE, Li L, Westermann AJ, Appenzeller S, Stapels DA, Schulte LN, et al. Single-cell RNA-seq
514 ties macrophage polarization to growth rate of intracellular Salmonella. Nat Microbiol. 2016;2:16206.
515 42. Eisele NA, Ruby T, Jacobson A, Manzanillo PS, Cox JS, Lam L, et al. Salmonella require the fatty
516 acid regulator PPARdelta for the establishment of a metabolic environment essential for long-term
517 persistence. Cell Host Microbe. 2013;14(2):171-82.
518 43. Park SH, Choi HJ, Yang H, Do KH, Kim J, Lee DW, et al. Endoplasmic reticulum stress-activated
519 C/EBP homologous protein enhances nuclear factor-kappaB signals via repression of peroxisome
520 proliferator-activated receptor gamma. J Biol Chem. 2010;285(46):35330-9.

521

522

bioRxiv preprint doi: https://doi.org/10.1101/2023.11.03.565559; this version posted November 3, 2023. The copyright holder for this preprint (which was not certified by peer review) is the author/funder, who has granted bioRxiv a license to display the preprint in perpetuity. It is made available under aCC-BY-NC-ND 4.0 International license.

523 **Figure Legends**

524 **Figure 1. *S.* Typhimurium activates the UPR *in vivo.*** RNA was extracted from the colon of S.
525 Typhimurium (SL1344) infected (10^8 cfu/mouse) and uninfected mice (C57BL/6) and analyzed by
526 qRT-PCR for expression of the ER stress markers *Xbp1* (A), *Hspa5* (B) and *Chop* (C). Data shown
527 as mean ± SEM with 6-10 mice per group. Ordinary one-way ANOVA followed by Dunnett's
528 multiple comparisons test. p value *<0.05, **<0.01, ***<0.001 and ****<0.0001 using GraphPad
529 PRISM.

530 **Figure 2. CHOP contributes to colonization, dissemination, and pathology during S.**
531 **Typhimurium infection.** Streptomycin-pretreated *Chop*$^{-/-}$ and *Chop*$^{+/-}$ littermate control mice were
532 infected with *S*. Typhimurium (SL1344, 10^8 cfu/mouse) and bacterial numbers were determined
533 in colon contents (A) and liver (B) at 24h, 48h and 72h post infection. (C) Total histopathology
534 scores for colon sections at 72h p.i. (D) Total neutrophil count. (E) Representative images of the
535 colon of *Chop*$^{-/-}$ and *Chop*$^{+/-}$ mice mock-treated or infected with S. Typhimurium for 72h. Data
536 shown as mean ± SEM or min to max with 6-10 mice per group. A and B; Multiple unpaired t tests.
537 C and D; unpaired t tests. p value *<0.05, **<0.01, ns (not significant) using GraphPad PRISM.

538 **Figure 3. *Chop*$^{-/-}$ mice have reduced cytokine expression.** RNA from the colon of infected and
539 uninfected *Chop*$^{-/-}$ and *Chop*$^{+/-}$ littermate control mice was extracted and analyzed by qRT-PCR
540 to determine the levels of *Nos2* (A), *Tnfa* (B), *Il1b* (C), *Kc* (D), and *Il23* (E) at 24h, 48h and 72h
541 post infection. Data shown as mean ± SEM with 5-8 mice per group. Unpaired t tests. p value
542 *<0.05, **<0.01, ***<0.001 and ****<0.0001, ns (not significant) using GraphPad PRISM.

543 **Figure 4. CHOP contributes to nitrate production resulting in a growth benefit for *S.***
544 **Typhimurium.** Streptomycin-pretreated *Chop*$^{-/-}$ and *Chop*$^{+/-}$ littermate control mice were infected
545 with a 1:1 mixture of wildtype *S*. Typhimurium SL1344 and *ΔnapAnarZnarG* (10^8 cfu/mouse). The

bioRxiv preprint doi: https://doi.org/10.1101/2023.11.03.565559; this version posted November 3, 2023. The copyright holder for this preprint (which was not certified by peer review) is the author/funder, who has granted bioRxiv a license to display the preprint in perpetuity. It is made available under aCC-BY-NC-ND 4.0 International license.

546 competitive index (CI) in the colon contents was determined 72h post infection. Data shown as
547 mean ± SEM with 9-10 mice per group. Unpaired t test. p value **<0.01 using GraphPad PRISM.
548 **Figure 5. CHOP expression in IECs does not contribute to resistance to S. Typhimurium**
549 **infections.** Streptomycin-pretreated *Chop*$^{\Delta IEC}$ and *Chop*^{flox} littermate control mice were infected
550 with *S*. Typhimurium (SL1344, 10^8 cfu/mouse) and cfus were determined in colon contents (A)
551 and liver (B) at 72hpi. (C) Total histopathology scores and (D) neutrophil counts in the colon at
552 72hpi. (E) *Nos2* mRNA levels in the colon. Data shown as mean ± SEM or min to max with 5-7
553 mice per group. (A and B) Mann-Whitney U test, (C-E) unpaired t tests, ns (not significant).
554 **Figure 6. CHOP deficient CD45+/CD11b+ colonic cells produce less iNOS.** Representative
555 flow plots of staining for CD11b and iNOS on cells isolated from colonic tissue of *S*. Typhimurium
556 infected mice at 72h p.i. (A). Percent of CD45+ live cells that are CD11b+/iNOS- (B) and
557 CD11b+/iNOS+ (C). Quantification of number of CD11b+/iNOS- cells (D) and CD11b+/iNOS+
558 cells (E). Data shown as mean ± SEM with 6 mice per group. Unpaired t tests. p value *<0.05,
559 ns (not significant) using GraphPad PRISM.

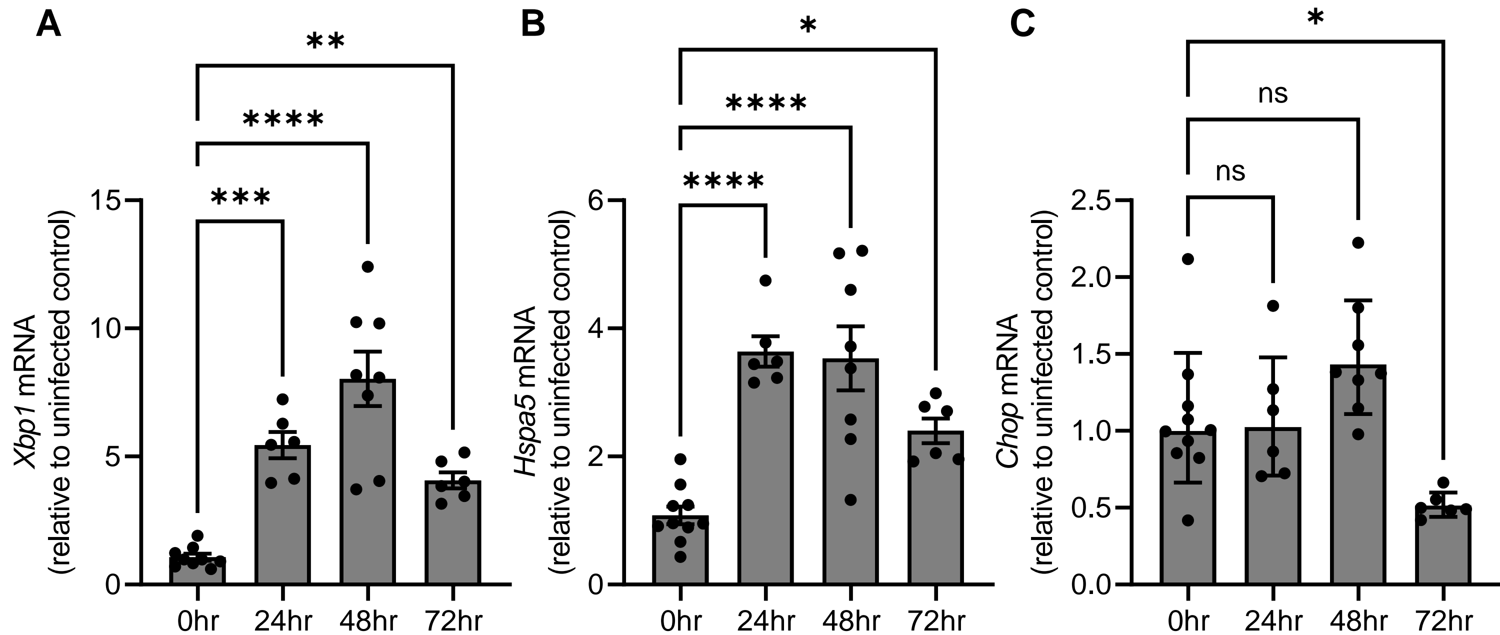

A
B
C
**
****
***
*
****
****
ns
ns
*
15
10
5
0
6
4
2
0
2.5
2.0
1.5
1.0
0.5
0.0
Xbp1 mRNA
(relative to uninfected control)
Hspa5 mRNA
(relative to uninfected control)
Chop mRNA
(relative to uninfected control)
0hr
24hr
48hr
72hr
0hr
24hr
48hr
72hr
0hr
24hr
48hr
72hr

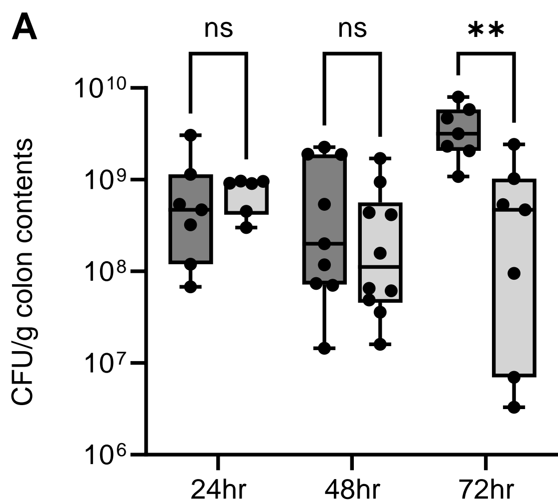
A
ns
ns
**
10^{10}
10^{9}
10^{8}
10^{7}
10^{6}
CFU/g colon contents
24hr
48hr
72hr

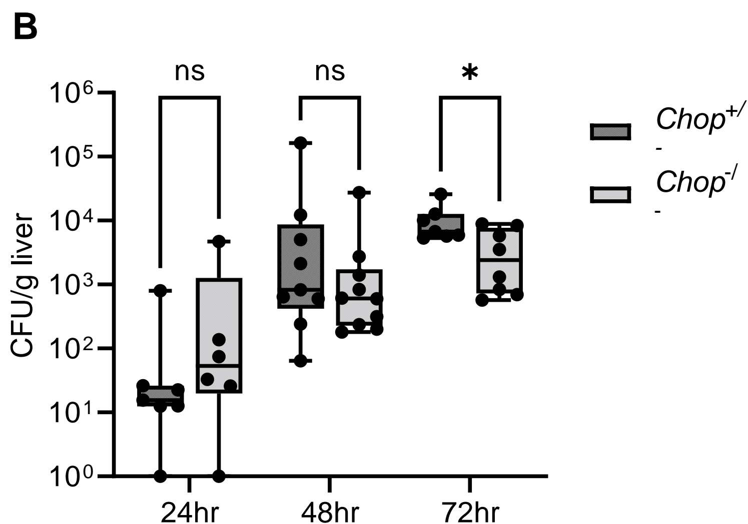
B
ns
ns
*
10^{6}
10^{5}
10^{4}
10^{3}
10^{2}
10^{1}
10^{0}
CFU/g liver
24hr
48hr
72hr
Chop+/-
Chop-/-

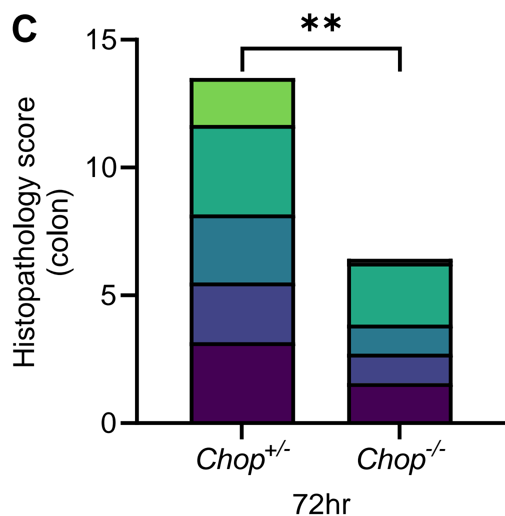
C
**
15
10
5
0
Histopathology score (colon)
Chop+/-
Chop-/-
72hr
Exudate
Epithelial Damage
Submucosal Edema
Infiltration MNC
Infiltration PMN

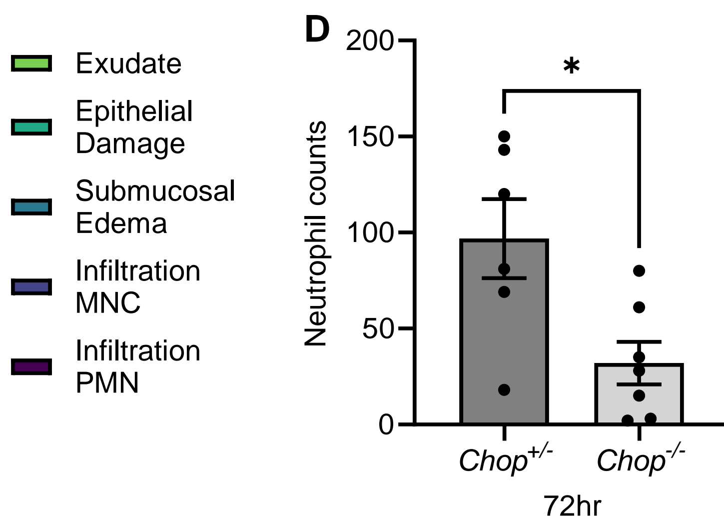
D
*
200
150
100
50
0
Neutrophil counts
Chop+/-
Chop-/-
72hr

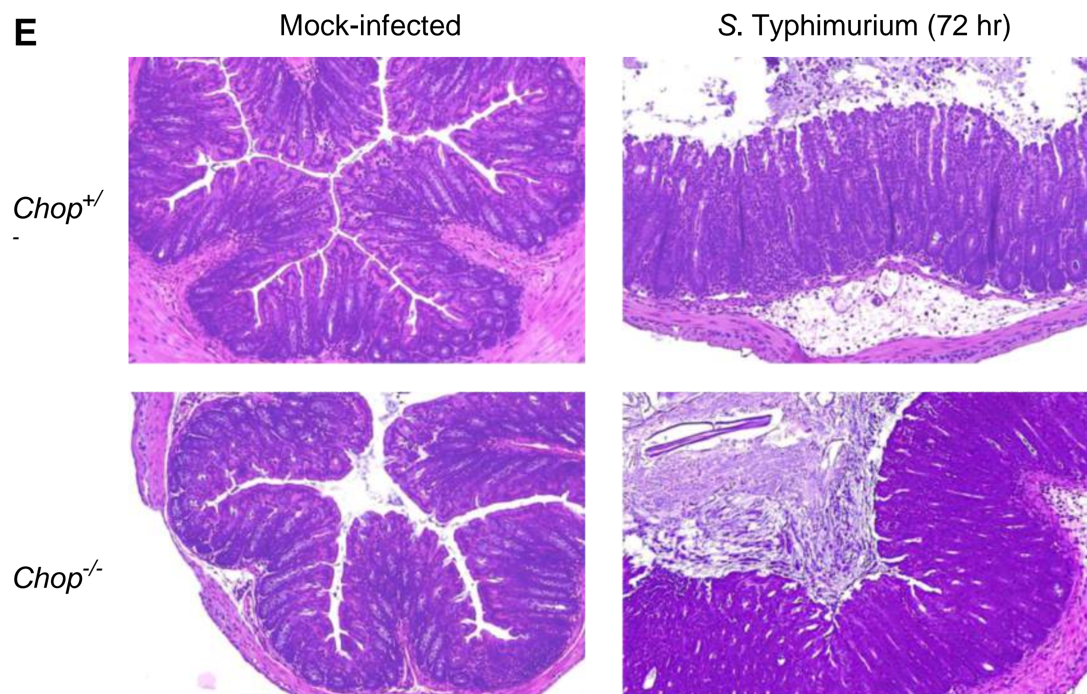
E
Mock-infected
S. Typhimurium (72 hr)
Chop+/-
Chop-/-

bioRxiv preprint doi: https://doi.org/10.1101/2023.11.03.565559; this version posted November 3, 2023. The copyright holder for this preprint (which was not certified by peer review) is the author/funder, who has granted bioRxiv a license to display the preprint in perpetuity. It is made available under aCC-BY-NC-ND 4.0 International license.

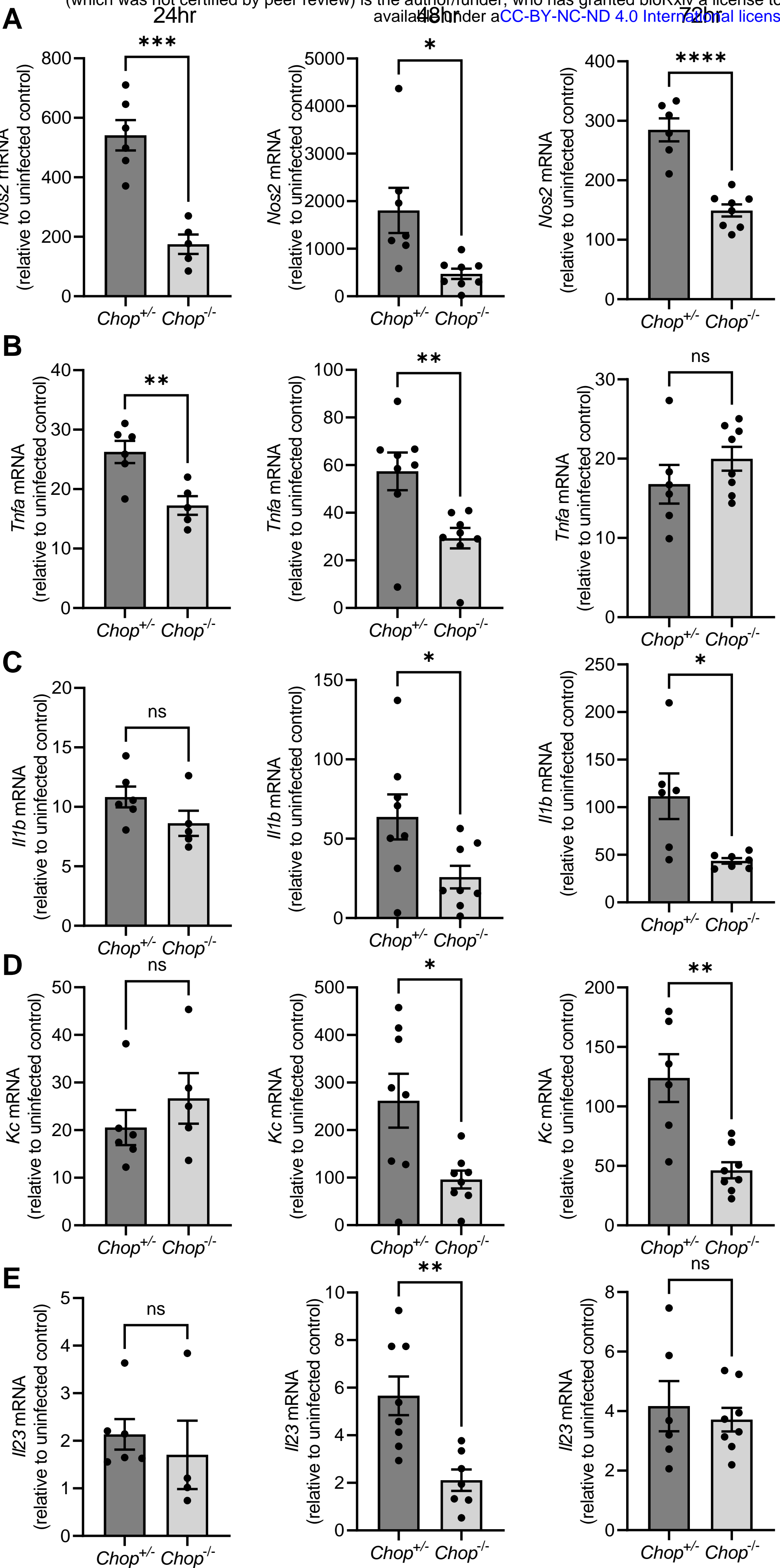

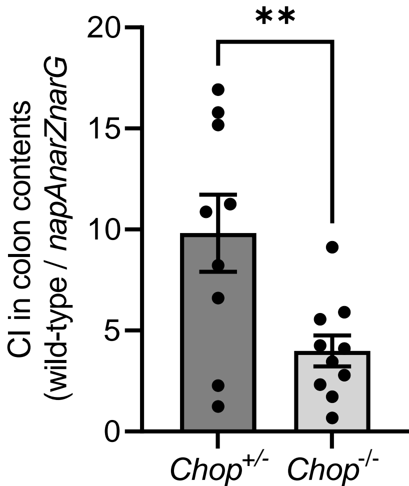
**
20
15
10
5
0
CI in colon contents
(wild-type / napAnarZnarG
Chop+/-
Chop-/-

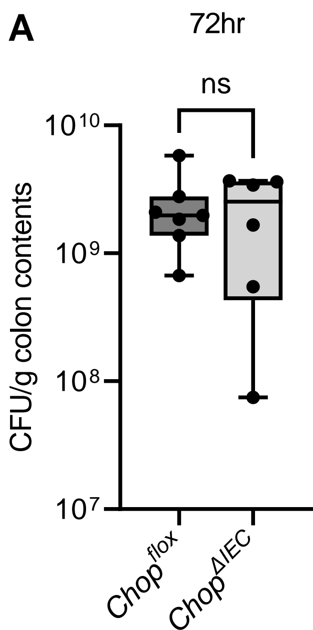
A
72hr
ns
10^{10}
10^9
10^8
10^7
CFU/g colon contents
Chop^flox
Chop^ΔIEC

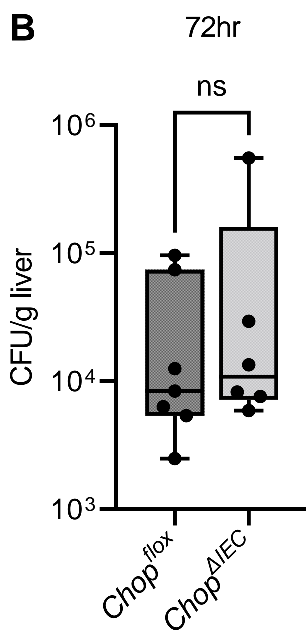
B
72hr
ns
10^6
10^5
10^4
10^3
CFU/g liver
Chop^flox
Chop^ΔIEC

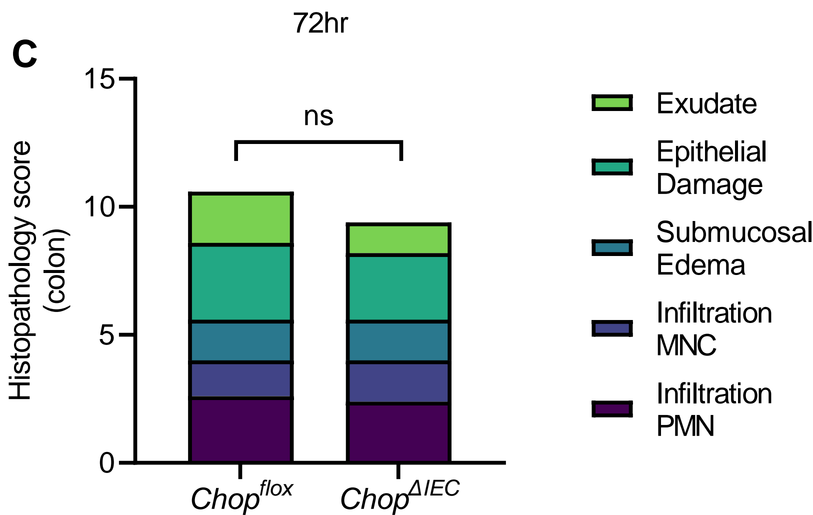
C
72hr
ns
15
10
5
0
Histopathology score (colon)
Chop^flox
Chop^ΔIEC
Exudate
Epithelial Damage
Submucosal Edema
Infiltration MNC
Infiltration PMN

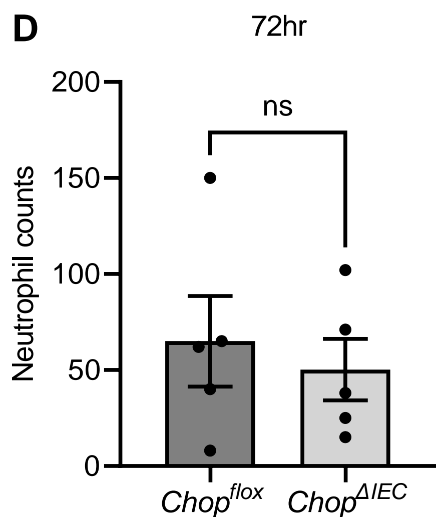
D
72hr
ns
200
150
100
50
0
Neutrophil counts
Chop^flox
Chop^ΔIEC

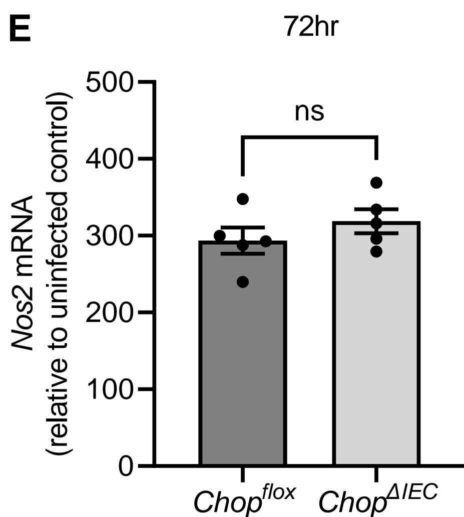
E
72hr
ns
500
400
300
200
100
0
Nos2 mRNA (relative to uninfected control)
Chop^flox
Chop^ΔIEC

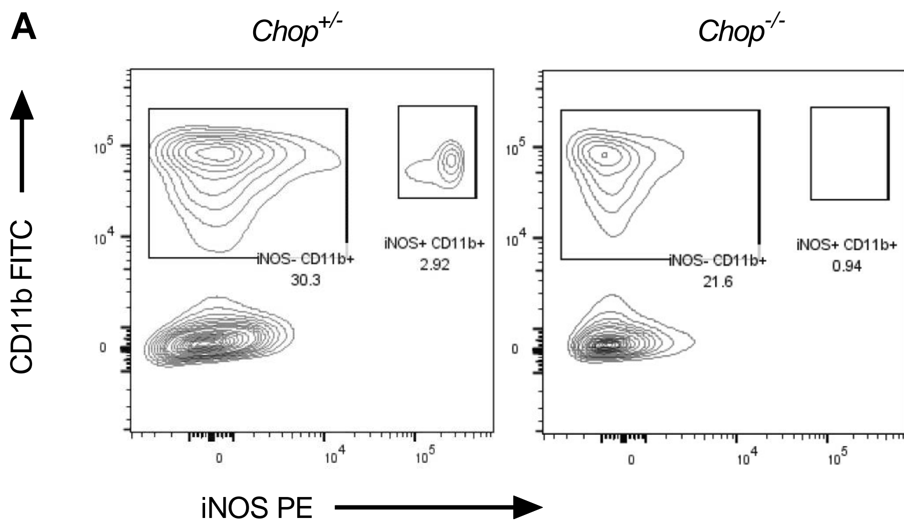
A
Chop+/-
Chop-/-
CD11b FITC
iNOS PE
iNOS- CD11b+
30.3
iNOS+ CD11b+
2.92
iNOS- CD11b+
21.6
iNOS+ CD11b+
0.94

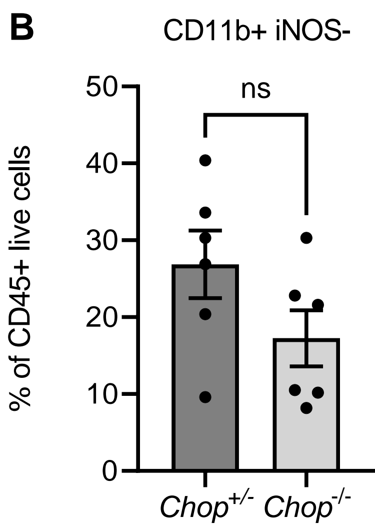
B
CD11b+ iNOS-
ns
% of CD45+ live cells
Chop+/-
Chop-/-

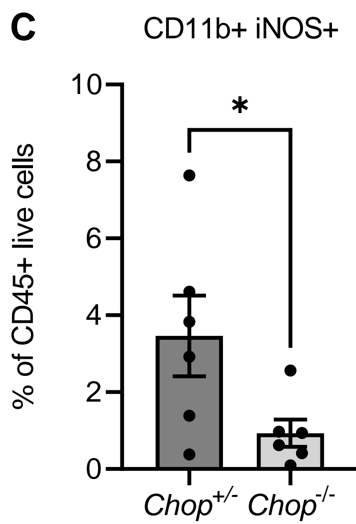
C
CD11b+ iNOS+
*
% of CD45+ live cells
Chop+/-
Chop-/-

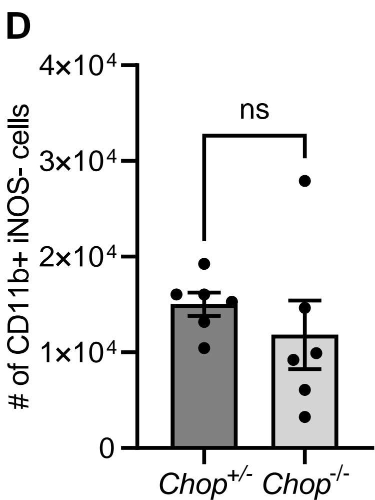
D
ns
# of CD11b+ iNOS- cells
Chop+/-
Chop-/-

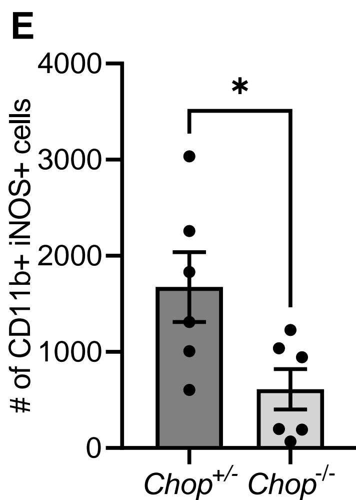
E
*
# of CD11b+ iNOS+ cells
Chop+/-
Chop-/-